https://doi.org/10.5194/essd-2025-378
Preprint. Discussion started: 8 September 2025

Open Access Earth System Science Data Discussions

A fused canopy height map of Italy (2004–2024) from spaceborne and airborne LiDAR, and Landsat via deep learning and Bayesian averaging

Authors

Yang Su [1, 2, 3], Nikola Besic [4], Xianglin Zhang [3], Yidi Xu [2], Saverio Francini [5], Giovanni D'Amico [6], Gherardo Chirici [7, 8], Martin Schwartz [2], Ibrahim Fayad [2], Sarah Brood [1], Agnes Pellissier-tanon [2], Ke Yu [2], Haotian Chen [9, 3], Songchao Chen [10], Alexandre d'Aspremont [1], Philippe Ciais [2]

Affiliations

[1] CNRS & Département d'Informatique, École Normale Supérieure – PSL, 45 Rue d'Ulm, 75005 Paris, France

[2] Laboratoire des Sciences du Climat et de l'Environnement, CEA CNRS UVSQ Orme des Merisiers, 91190 Gif-sur-Yvette, France

[3] Université Paris-Saclay, AgroParisTech, INRAE, UMR ECOSYS, 91120 Palaiseau, France

[4] IGN, ENSG, Laboratoire d'inventaire forestier (LIF), 54000 Nancy, France

[5] Department of Science and Technology of Agriculture and Environment (DISTAL), University of Bologna, 40126 Bologna, Italy

[6] Department of Agriculture, Food, Environment and Forestry, Università degli Studi di Firenze, Via San Bonaventura, 13, 50145 Firenze, Italy

[7] Fondazione per il Futuro delle Città, Florence, Italy

[8] CNR Istituto dei Sistemi Complessi, Sesto Fiorentino (Florence), Italy

[9] Institute of Crop Sciences, Chinese Academy of Agricultural Sciences / Key Laboratory of Crop Physiology and Ecology, Ministry of Agriculture and Rural Affairs of China, Beijing 100081, China

[10] College of Environmental and Resource Sciences, Zhejiang University, 310058 Hangzhou, China

Corresponding Author

Yang Su yang.su@ens.fr +33 1 89 10 07 67 École Normale Supérieure – PSL

Abstract

Forests are vital for the carbon sequestration, biodiversity conservation, and climate regulation, making the precise and continuous monitoring of forest structure attributes such as canopy height essential. Here we present a two decades long (2004–2024), 30m resolution annual canopy height dataset for Italy, developed using a time-series deep learning framework that integrates Landsat optical imagery with LiDAR observations. Two UNET models were independently trained using canopy height reference data from airborne laser scanning (ALS) and NASA's Global Ecosystem Dynamics Investigation (GEDI) spaceborne LiDAR mission. Annual canopy height predictions from each model were fused using Bayesian Model Averaging (BMA) to enhance spatial consistency and temporal continuity. Validation against ground-based measurements from the Italian National Forest Inventory (NFI) demonstrated high predictive accuracy (mean absolute error = 3.98 m). To further evaluate the utility of our dataset, we derived a canopy height change-based disturbance product and validated it against observed events (mean precision = 0.64 for 2005–

https://doi.org/10.5194/essd-2025-378
Preprint. Discussion started: 8 September 2025

Open Access Earth System Science Data Discussions

2016). In addition, we assessed post-disturbance recovery by monitoring canopy height regrowth in areas affected during 2004–2005, tracking changes annually through 2024 across various Italian biomes. Our results highlight the importance of integrating multi-source remote sensing data with deep learning and Bayesian data fusion for monitoring forest structural dynamics. The final dataset is publicly available via Zenodo and provides a reproducible and scalable resource to support forest research, ecological monitoring, and climate-related policy-making.

1. Introduction

Forests play a central role in regulating the Earth system through carbon sequestration, climate moderation, water cycling, and biodiversity conservation (Shukla et al., n.d.). Quantifying forest structure—particularly canopy height—is critical for estimating forest biomass, understanding ecosystem dynamics, and informing forest management and climate mitigation strategies (Chave et al., 2014). Despite its importance, accurate and long-term canopy height and height change data remain scarce, particularly at high spatial resolutions. In Italy, where forests range from Mediterranean woodlands to alpine coniferous ecosystems (Selvi et al., 2023), spatially detailed and temporally continuous monitoring is crucial for assessing ecological change and supporting sustainable forest management. Yet, most existing canopy height datasets over Italy represent only single-year snapshots, lacking the temporal depth necessary to capture forest dynamics over time (Lang et al., 2023; Pauls et al., 2024; Potapov et al., 2021).

Recent advances in remote sensing and deep learning have substantially enhanced our capacity to monitor forest structural attributes such as canopy height (Lang et al., 2023; Pauls et al., 2024). Increasingly, studies have combined discrete LiDAR measurements with continuous satellite imagery to generate spatially explicit canopy height maps over large areas (Fayad et al., 2024; Hansen et al., 2013a; Lang et al., 2023; Pauls et al., 2024; Potapov et al., 2021; Rajab Pourrahmati et al., 2024; Schwartz et al., 2023; Su et al., 2025). Deep learning techniques, such as convolutional neural networks, have further improved the accuracy and scalability of these approaches by learning complex, multi-scale spatial patterns from large training datasets (Fayad et al., 2024; Lang et al., 2023; Pauls et al., 2024; Rajab Pourrahmati et al., 2024; Schwartz et al., 2023; Su et al., 2025).

Among the available satellite platforms, the Landsat missions are the only ones providing four decades of 30m-resolution optical multispectral imagery with global coverage and frequent temporal observations (Crawford et al., 2023; Kovalskyy and Roy, 2013; Roy et al., 2014; Wulder et al., 2022). For LiDAR sources, airborne laser scanning (ALS) is widely regarded as one of the most accurate methods for estimating canopy height, providing high spatial resolution and accurate structural information (Wulder et al., 2012) (with data available from 2004 to 2017 in Italy (Montaghi et al., 2013)). However, the operational costs of ALS campaigns limit their spatial and temporal availability, especially at national or continental scales (Coops et al., 2021). In contrast, the Global Ecosystem Dynamics Investigation (GEDI), a spaceborne LiDAR mission, offers a more recent (with operational data available from 2019 in Italy) and globally distributed dataset, capturing canopy height at a large scale (Dubayah et al., 2020; Potapov et al., 2021). While GEDI offers greater spatial coverage than ALS, its temporal coverage is shorter and the footprint-based measurements remain sparse.

Critically, the capability of large-scale monitoring the vertical structure of forests opens new possibilities for both forest disturbance detection and post-disturbance recovery monitoring (Francini et al., 2022) , which is more critical than ever undercurrent climate change scenarios (Palahí et al., 2021) . While forest disturbances have traditionally been monitored using optical satellite data (Hansen et al., 2013b; Hermosilla et al., 2015; Kennedy et al., 2010) , and several classification products have recently been developed for Italy at varying temporal resolutions (Francini et al., 2020, 2021, 2023), there remains a significant gap in the availability of maps that track changes in canopy height over time. Large-scale, long-term predictions of forest canopy height have the potential to fill this gap by enabling the creation of height change maps, which reveal structural transformations that are often invisible to optical sensors. These maps provide

https://doi.org/10.5194/essd-2025-378
Preprint. Discussion started: 8 September 2025

valuable complementary information to traditional disturbance products, offering enhanced insights into disturbance events, post-disturbance recovery trajectories, and forest resilience—critical components for understanding forest dynamics under changing environmental conditions.

In this study, we present a long-term (2004–2024), 30m resolution annual map of maximum canopy height for Italy. Our workflow coupled the ALS and GEDI data with Landsat multispectral data in a deep-learning framework: one UNET model (Ronneberger et al., 2015) was trained with ALS–Landsat pairs from 2004–2017, and a second with GEDI–Landsat pairs from 2019–2023. Annual canopy height predictions from 2004 to 2024 were generated independently using each model. To enhance consistency and accuracy across space and time, we applied Bayesian Model Averaging (BMA) (Hoeting et al., 1999) to fuse these ALS-Landsat and GEDI-Landsat based canopy height maps, with the measurements from the Italian National Forest Inventory (NFI) guiding the spatially adaptive weights. The resulting dataset offers a harmonized 30m-resolution time series record of canopy height across Italy, serving as a valuable tool for forest monitoring, carbon stock assessment, and land-use change analysis. We demonstrate its applicability by deriving a disturbance product based on canopy height change and tracking post-disturbance regrowth in areas affected during 2004–2005 across different Italian biomes (**Figure S1**). Our results highlight the utility of this dataset as a robust baseline for assessing forest structural dynamics in response to climate change and anthropogenic influences.

2. Data

2.1 Remote Sensing Data

Landsat surface reflectance products from the Thematic Mapper (TM, Landsat 5) (Crawford et al., 2023; Kovalskyy and Roy, 2013; USGS Landsat 5 Level 2, Collection 2, Tier 1, 2025; Wulder et al., 2022), Enhanced Thematic Mapper Plus (ETM+, Landsat 7) (Kovalskyy and Roy, 2013; USGS Landsat 7 Level 2, Collection 2, Tier 1, 2025), and Operational Land Imager (OLI, Landsat 8) (Roy et al., 2014; USGS Landsat 8 Level 2, Collection 2, Tier 1, 2025) were used as the primary optical inputs for canopy height modeling over the 2004–2024 period. All imagery was sourced from the USGS Collection 2, Tier 1 Level-2 Surface Reflectance datasets, which include atmospheric correction and quality assurance bands for cloud and shadow masking (Landsat Algorithms, 2025; USGS Landsat 5 Level 2, Collection 2, Tier 1, 2025; USGS Landsat 7 Level 2, Collection 2, Tier 1, 2025; USGS Landsat 8 Level 2, Collection 2, Tier 1, 2025).

Given the evolution of the Landsat program and sensor transitions (Vermote et al., 2016; Wulder et al., 2016), we split the data processing pipeline into two distinct periods: 2004–2012 and 2013–2024. For the first period (2004–2012), annual median composites were generated from Landsat 5 and 7. Since both sensors have spectral response characteristics that differ from the more recent Landsat 8, a harmonization step was necessary to ensure consistency across the full time series (Roy et al., 2016). We applied a linear transformation to normalize TM and ETM+ surface reflectance values to the OLI spectral space using the available slope and intercept coefficients (Landsat ETM+ to OLI Harmonization, 2025; Roy et al., 2016). The same transformation was applied to both Landsat 5 and 7, a common approach in long-term forest monitoring studies due to their comparable spectral bands and the need for alignment with the OLI reference system (Landsat ETM+ to OLI Harmonization, 2025; KC et al., 2021; Roy et al., 2014, 2016; Savage et al., 2018; Vogeler et al., 2018). Quality assessment and masking were conducted using the QA bands provided in Collection 2 Level-2 products (USGS Landsat 5 Level 2, Collection 2, Tier 1, 2025; USGS Landsat 7 Level 2, Collection 2, Tier 1, 2025; USGS Landsat 8 Level 2, Collection 2, Tier 1, 2025). From the QA_PIXEL band, we excluded pixels flagged as Fill (bit 0), Cirrus (bit 2; populated for OLI only), Dilated Cloud (bit 1), Cloud (bit 3) and Cloud Shadow (bit 4). In addition, pixels flagged as radiometrically saturated in any band (QA_RADSAT $\neq 0$) were removed. After QA filtering, we then computed vegetation and water-related indices, including Normalized Difference Vegetation Index (NDVI), Enhanced Vegetation Index (EVI), Land Surface Water Index (LSWI) and Normalized Difference Water Index (NDWI).

https://doi.org/10.5194/essd-2025-378
Preprint. Discussion started: 8 September 2025

For the second period (2013–2024), data availability was extended with the launch of Landsat 8, which provides improved radiometric performance and refined spectral band definitions (Roy et al., 2014). OLI imagery was processed directly with the above-mentioned QA-based masking, and no reflectance normalization was required. Data from Landsat 7 continued to be harmonized to match OLI reflectance values, ensuring spectral consistency across the entire time series (Landsat ETM+ to OLI Harmonization, 2025; Roy et al., 2016). For each year, an annual median composite was generated from all valid cloud-free images from both Landsat 7 and 8. Spectral indices were calculated using the same formulas as in the earlier period to ensure comparability across time. The script for downloading the Landsat data is accessible via Figshare (Code used in the study - "A fused canopy height map of Italy (2004–2024) from spaceborne and airborne LiDAR, and Landsat via deep learning and Bayesian averaging ", 2025). Although Landsat 9, launched in late 2021, provides data with nearly identical spectral and radiometric properties to Landsat 8 (Kaewmanee et al., 2023; Xu et al., 2023a), it was not incorporated in this study as the strong sensor similarity between OLI and OLI-2, the inclusion of Landsat 9 would not materially change the annual median composites or downstream canopy height predictions.

To characterize topographic variation across Italy, we used the Advanced Land Observing Satellite (ALOS) World 3D 30 m Digital Surface Model (AW3D30), provided by the Japan Aerospace Exploration Agency (JAXA) (Tadono et al., 2014, 2016; Takaku et al., 2014, 2016). The AW3D30 dataset offers global elevation data at a 30 m spatial resolution, derived from PRISM stereo imagery. We extracted the “DSM” band, which represents surface elevation including vegetation and built structures. And to support terrain-related analysis of canopy height patterns, we derived slope information using the ee.Terrain.slope() function (ee.Terrain.slope, 2025) applied to the AW3D30 mosaic. The code for downloading digital terrain information is available via Figshare (Code used in the study - "A fused canopy height map of Italy (2004–2024) from spaceborne and airborne LiDAR, and Landsat via deep learning and Bayesian averaging ", 2025).

2.2 LiDAR Reference Data

2.2.1 Airborne Laser Scanning Data (ALS)

ALS data used in this study were sourced from various national and regional airborne survey campaigns conducted between 2004 and 2017 across Italy (D’Amico et al., 2021; Montaghi et al., 2013). The datasets were acquired using different airborne lidar sensors, most commonly Optech ALTM systems (Gemini, 3032, 3033, and 3100; Teledyne Optech, Canada), Riegl LMS sensors (Q560, Q680i; RIEGL Laser Measurement Systems, Austria), Leica ALS50-II (Leica Geosystems, Switzerland), and TopoSys Falcon II (Germany) (**Table S1**). These sensors are full-waveform or discrete-return lidar systems operating in the near-infrared (NIR) spectrum (**Table S1**), which is standard for vegetation and topographic mapping (Budei et al., 2018; Wagner et al., 2008).

Flight characteristics varied widely across surveys. Flight altitudes ranged from 180 m to 4700 m above ground level, while point density ranged from 0.4 to over 5 pulses per square meter, and spatial resolution from 1 m to 5 m (**Table S1**). However, additional details on flight speed and overlaps were not consistently available for all surveys. When available, the lidar system settings used a forward overlap of 50–60% and a side overlap of 20–30%, with aircraft speeds generally between 150 and 250 km/h depending on altitude and swath width (Pirotti, 2010). These acquisition parameters are designed to ensure adequate point density and minimize occlusion effects in forested areas. Vertical accuracy for these ALS datasets typically ranges from 10 to 30 cm RMSE, and horizontal accuracy from 20 to 50 cm, depending on sensor type, flight altitude, and GPS/IMU quality (Optech, n.d.).

The temporal distribution of the datasets reflects various institutional objectives: some surveys were created for hydraulic risk assessment (e.g., MATTM acquisitions along rivers and coastlines), others for regional environmental monitoring (e.g., Piemonte, Trentino, Valle d’Aosta), and some for local forest or ecological studies (e.g., Bosco Fontana). The seasonal timing of the acquisitions is not consistently reported across providers. However, available metadata and project documentation show that most campaigns took place

https://doi.org/10.5194/essd-2025-378
Preprint. Discussion started: 8 September 2025

during late spring to summer months, when cloud-free and leaf-on conditions support high-quality data collection (Montaghi et al., 2013; Pirotti, 2010). Leaf-on conditions maximize canopy detection but may reduce ground return availability, while occasional leaf-off campaigns improve ground model accuracy at the cost of slightly lower canopy height estimates. In several regions, multitemporal acquisitions are available due to overlapping campaigns, such as MATTM and regional surveys, especially in Liguria, Valle d'Aosta, Molise, Piemonte, Trentino-Alto Adige, and Basilicata. Depending on the provider, the delivered products ranged from raw point clouds to pre-processed Digital Terrain Models (DTMs) and Digital Surface Models (DSMs) (**Table S1**).

Despite their high precision, the use of ALS data is constrained by the high cost of acquisition and the lack of systematic temporal and spatial coverage. As a result, ALS availability is fragmented across both time and geography. ALS data were available for a total area of approximately 16.86 million hectares, covering about 56% of Italy's national territory (D'Amico et al., 2021) (**Figure S2b**). To ensure compatibility with the Landsat-based modeling framework, the ALS canopy height measurements were aggregated to a 30 m spatial resolution. Within each 30 m pixel, the maximum canopy height was extracted from the underlying 1 m ALS measurements, yielding a consistent reference layer for model training and validation. Given the high vertical accuracy of ALS (~10–30 cm RMSE (Optech, n.d.)), resampling to 30 m is expected to contribute only minor additional error, although local variability in acquisition settings (altitude, density, season) may explain part of the residual uncertainty in model validation.

2.2.2 Global Ecosystem Dynamics Investigation Data (GEDI)

GEDI canopy height data were retrieved via GEE from the collection labeled "LARSE/GEDI/GEDI02_A_002_MONTHLY", which corresponds to the GEDI Version 2 Level 2A Geolocated Elevation and Height Metrics Product. Version 2 includes improved waveform geolocation algorithms and calibration relative to Version 1, leading to enhanced vertical accuracy and reduced geolocation bias (Dubayah et al., 2021). Reported accuracy assessments indicate an average horizontal geolocation error of 10.2 m and an elevation error of approximately 17.8 cm over gentle terrain (Xu et al., 2023b).

We extracted data spanning 2019 to 2023, using the Relative Height at 98% energy return (RH98) metric to represent maximum canopy height, which match better with the NFI maximum heights (Besic et al., 2025; Su et al., 2025). To ensure high data quality, we applied a series of rigorous filters (Schwartz et al., 2023; Su et al., 2025). First, to minimize errors associated with solar contamination, we included only nighttime acquisitions, defined as observations where solar elevation was below 0 degrees. Second, to reduce the influence of terrain-induced uncertainty—known to affect LiDAR signal accuracy on steep slopes (Kutchartt et al., 2022), we limited the inclusion of GEDI data to the regions with a slope of no more than 10 degrees. To further avoid geolocation artifacts near forest – non-forest boundaries, e excluded GEDI footprints within 25 m of forest edges, based on a morphological edge filter (focal_max) applied to the ESA WorldCover 2020 tree cover classification (ESA WorldCover 10 m 2021 v200, 2024). This additional buffer helped mitigate misclassification and spatial mismatch errors (Schleich et al., 2023). After all filtering steps, a total of 1,485,449 GEDI footprints were retained for analysis (**Figure S2a**). Although GEDI data are natively available at a 25 m spatial resolution, we resampled the RH98 values to 30 m to align with the Landsat data used for model input. The code for downloading GEDI canopy height data is available via Figshare (Code used in the study - "A fused canopy height map of Italy (2004–2024) from spaceborne and airborne LiDAR, and Landsat via deep learning and Bayesian averaging ", 2025).

2.3 Ground Validation Data

2.3.1 Canopy Height Data from National Forest Inventory (NFI)

The NFI data used in this study were obtained from the Italian National Forest Inventory 2015 campaign (INFC2015) (Gasparini and Di Cosmo, 2015; Gasparini and Floris, 2022; National Inventory of Forests and forest Carbon pools - INFC, 2025), which was designed to provide consistent, spatially detailed

https://doi.org/10.5194/essd-2025-378
Preprint. Discussion started: 8 September 2025

information on forest structure and biomass across the country (Gasparini and Di Cosmo, 2015). INFC2015 employed a three-phase stratified sampling approach (Gasparini and Di Cosmo, 2015; Gasparini and Floris, 2022). In the first phase, a systematic grid of 1 km × 1 km cells is established over the entire national territory. Within each cell, a single point is randomly selected and classified using high-resolution imagery in land cover types. The second phase, carried out on a subsample of forested points identified in the first phase, involves a qualitative survey that refines forest type classification. In the third phase, a random subsample of 6,894 second phase points is selected for field survey. Each point was surveyed in the field to measure forest attributes within nested circular design plots, centered on the selected points. Trees with diameter at breast height (DBH) ≥ 4.5 cm were measured within a 4m radius subplot (approximately 50.27 m2), while trees with DBH ≥ 9.5 cm were recorded within a larger 13 m radius subplot (approximately 530 m2). The 13m subplot was also used to collect measurements of tree height, increment cores, stumps, and lying deadwood. For each tree, species identity, canopy height, and health status were recorded, enabling estimation of volume and biomass through species-specific allometric models. Beyond tree-level attributes, the campaign also assessed forest regeneration, dead organic matter, and land use change, with a focus on maintaining methodological consistency with the earlier INFC2005 inventory and aligning with international forest monitoring standards (Gasparini and Floris, 2022).

In our analysis, we initially collected 217,421 records of canopy height for individual living trees from forested sites surveyed in the INFC2015 dataset. Since each site included multiple tree measurements, we selected the highest canopy height recorded at each location (based on geographic coordinates) to represent the site-level maximum After processing, a total of 6,894 field observations were retained for model validation (**Figure S2c**).

2.3.2 Reference Data for Forest Disturbance

The reference data (Monitoring clearcutting and subsequent rapid recovery in Mediterranean coppice forests with Landsat time series. Zenodo repository. [dataset]., 2025; Chirici et al., 2020; Francini et al., 2021, 2022) were derived through manual interpretation of Landsat imagery since 1999, following an approach comparable to the TimeSync protocol (Cohen et al., 2010). Interpreters delineated the spatial boundaries of clearcuts and recorded the corresponding year of harvest, using a minimum mapping unit of 0.1 ha. In addition to Landsat imagery, high-resolution aerial photographs accessed via a Web Map Service (WMS) were used to support interpretation. Field visits were conducted in coordination with local forest authorities to confirm harvest timing and extent. After quality control procedures (Chirici et al., 2020), the resulting geodatabase was deemed an accurate record of clearcut location and timing from 1999 to 2016 (Monitoring clearcutting and subsequent rapid recovery in Mediterranean coppice forests with Landsat time series. Zenodo repository. [dataset]., 2025; Chirici et al., 2020).

3. Method

Our workflow began by developing two UNET-Landsat based canopy height models using ALS and GEDI data, respectively (**Figure S3**). Each model was used to generate annual 30 m resolution canopy height maps across Italy from 2004 to 2024 (**Figure 1b**). To integrate their complementary strengths, we applied Bayesian Model Averaging (BMA) to fuse the predictions (**Figure 1a**), producing a harmonized, spatially consistent, and temporally continuous canopy height dataset. To demonstrate its utility, we used the annual maps to identify canopy disturbances based on interannual height losses and analyzed post-disturbance recovery patterns across Italian biomes over the two-decade period. A detailed description of the methods is provided in the subsequent sections.

https://doi.org/10.5194/essd-2025-378
Preprint. Discussion started: 8 September 2025

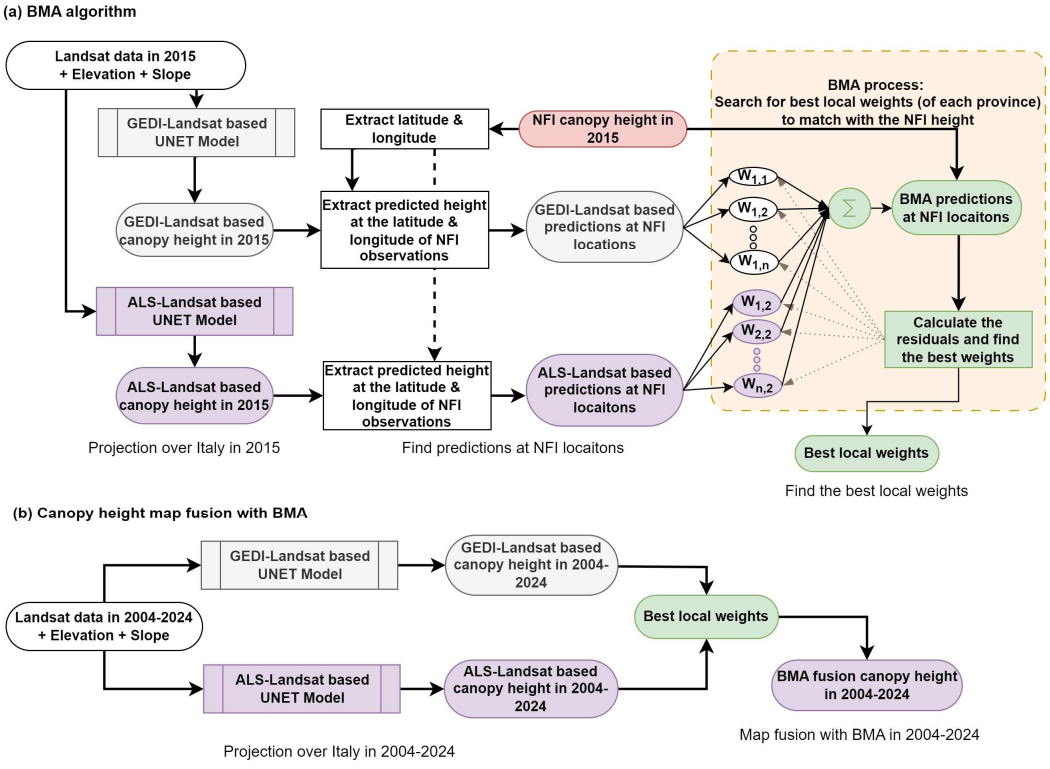

Figure 1 | Algorithm of Bayesian Model Averaging. *Plot a is the Flow chart of to search for the best local weights that can be used in BMA. Landsat imagery from 2015, combined with elevation and slope data, was input into both the GEDI-Landsat and ALS-Landsat UNET models to generate canopy height predictions across Italy. Predicted heights at NFI plot locations were extracted from both models and compared with observed NFI canopy heights. The BMA procedure (right panel) then optimized local weights for each province by minimizing the residuals between model predictions and NFI reference values. These weights were subsequently used to fuse the two UNET model outputs, ensuring accurate and region-specific canopy height estimates. Plot b is the workflow for generating the final canopy height product through BMA fusion from 2004 to 2024. Annual Landsat imagery, along with elevation and slope data, was used as input to two trained UNET models: one based on ALS reference data and the other on GEDI. Each model produced annual canopy height predictions across Italy. These predictions were then fused using spatially optimized BMA weights—previously derived from comparison with NFI reference data—to produce a temporally consistent, high-resolution canopy height dataset for the full 2004–2024 period.*

3.1 Canopy height mapping model

3.1.1 Model workflow

A UNET deep learning architecture, a fully convolutional neural network originally developed for biomedical image segmentation (Ronneberger et al., 2015), was employed to estimate annual canopy height across Italy from 2004 to 2024 at 30 m resolution. Characterized by its distinctive U-shaped structure, the UNET architecture is able to capture both global context and fine-grained spatial detail, making it particularly well-suited for remote sensing tasks. It facilitates the analysis of images at different scales, effectively capturing the spatial hierarchy and the relationship between adjacent pixels, even with limited

https://doi.org/10.5194/essd-2025-378
Preprint. Discussion started: 8 September 2025

297 data (Solórzano et al., 2021). This enables UNET to effectively identify and segment complex land cover
298 features such as forests, croplands, grasslands, human-built environments and lakes (Zhu et al., 2017). This
299 feature is particularly valuable for detecting canopy heights in various types of landscapes (Schwartz et al.,
300 2023).

301 To effectively model both spatial and temporal patterns of forest structure, we integrated ALS- or GEDI-
302 derived canopy height measurements from all available years with temporally corresponding Landsat
303 imagery during the training phase. Each canopy height reference point was matched with satellite input data
304 from the same acquisition year, ensuring that the model learned from consistent and synchronous
305 observations. This temporal alignment allowed the UNET models not only to recognize spatial patterns—
306 such as texture, structure, and contextual cues related to vegetation—but also to learn interannual changes
307 in canopy height. By incorporating this temporal dimension into the training process, the models gained the
308 ability to detect and generalize patterns of canopy growth, degradation, and regeneration over time, making
309 the approach well-suited for generating long-term, consistent canopy height estimates for forest monitoring.

310 The model architecture consisted of five down sampling and four up sampling blocks with skip connections,
311 batch normalization, and ReLU activation functions (Ronneberger et al., 2015). Each convolutional layer
312 used a 3×3 kernel size, and max-pooling was applied during down sampling to reduce spatial dimensions
313 (Ronneberger et al., 2015). The final output layer consisted of a single channel with a linear activation
314 function to predict continuous canopy height values.

315 ***3.1.2 Training, validation and testing for ALS-Landsat and GEDI-Landsat based UNET models***

316 In our implementation, the UNET takes as input a multi-channel image stack composed of 6 Landsat surface
317 reflectance bands, 2 digital terrain bands, and 4 vegetation indices including NDVI, EVI, LSWI and NDWI.
318 The inclusion of these indices aims to improve the interannual stability of the model outputs and mitigate
319 the effects of noise caused by year-to-year quality variability in satellite observations, which can be
320 influenced by factors such as cloud cover, atmospheric conditions, and shadow effects in time-series
321 imagery (Zhu and Woodcock, 2012). Each input tile corresponds to a 1000×1000 pixels (30km×30km)
322 patch with those 12 bands. To increase data diversity and improve model robustness, each tile was randomly
323 cropped into smaller 256×256-pixel patches prior to being fed into the model (Zheng et al., 2020). To
324 enhance generalization and prevent overfitting, batch normalization and dropout regularization were
325 applied throughout the network. Dropout randomly disables a subset of neurons during training, effectively
326 performing model averaging and reducing overfitting risk (Srivastava et al., 2014). And the mean absolute
327 error (MAE) loss function was used to optimize the model by minimizing the difference between predicted
328 and observed canopy height values (Schwartz et al., 2023). The detailed procedure for training, validating,
329 and testing our canopy height models was outlined in **Figure S3**. The detailed model structure and model
330 parameters can be found in **Table S1** and **Table S2**.

331 In this work, the UNET models were trained separately on ALS-derived or GEDI-derived canopy height
332 labels depending on the available time period. While the structure of both models remains identical, the
333 difference lies in the reference data employed. GEDI data provide extensive spatial coverage each year, yet
334 it does not provide spatially continuous height measurements due to its configuration and spanning from
335 2019 to 2023. Conversely, ALS data offer smaller yearly spatial coverage, but with a significantly higher
336 data density, and spanning from 2004 to 2017. Each dataset was randomly split into 3 parts at the input
337 patch level, 75% were assigned to the training set, 5% were utilized to the validation set for monitoring the
338 training progress of the UNET models (with training stopping once the validation loss converges), and the
339 remaining 20% were reserved as the out-of-box testing set to evaluate the final models' performances
340 (**Figure S4**). Model performance was quantified using three metrics: MAE, Root Mean Squared Error
341 (RMSE), and Coefficient of Determination (R^2).

342 **3.2 Model fusion with Bayesian Model Averaging (BMA)**

343 ***3.2.1 BMA description***

https://doi.org/10.5194/essd-2025-378
Preprint. Discussion started: 8 September 2025

The two UNET models developed in this study were trained on distinct reference datasets—ALS (2004–2017) and GEDI (2019–2023)—each characterized by different spatial and temporal properties. To harness the complementary strengths of both models and generate a spatially complete and temporally consistent canopy height dataset for Italy from 2004 to 2024, we adopted a Bayesian Model Averaging (BMA) fusion framework (Besic et al., 2025; Duan et al., 2007; Hoeting et al., 1999) (**Figure 1a**).

BMA is a probabilistic ensemble technique that combines predictions from multiple models by assigning weights based on their relative predictive performance (Hoeting et al., 1999). Under the BMA framework, it is assumed that each model's predictive error follows a Gaussian distribution centered around the true value. The posterior probability of each model—used as its weight—is computed based on how well the model's predictions align with a reference dataset (in our case, the Italian NFI data in 2015). This allows BMA to effectively quantify uncertainty and balance the strengths of different models (Besic et al., 2025; Chen et al., 2020; Duan et al., 2007; Hoeting et al., 1999).

In our implementation, BMA was used to compute a weighted average of ALS-Landsat and GEDI-Landsat based canopy height predictions at the provincial level. Italy comprises 107 provinces, and the optimal weights for each province were derived by comparing the model outputs at NFI plot locations within that specific province for the year 2015 against the corresponding observed canopy height measurements (**Figure S5**). This approach enables spatially adaptive weighting: in regions where one model underperforms, such as areas without ALS coverage or mountainous regions where GEDI accuracy may degrade (Kutchartt et al., 2022), the other model receives greater weight in the final fusion.

Mathematically, the fused canopy height H_{BMA} can be written as:

$$H_{BMA} = w_{ALS,\ province\ i} \times H_{ALS} + w_{GEDI,\ province\ i} \times H_{GEDI}$$

Where H_{ALS} and H_{GEDI} are the predicted canopy heights from ALS-Landsat and GEDI-Landsat based model, respectively. The weight $w_{ALS,\ province\ i}$ and $w_{GEDI,\ province\ i}$ are the corresponding optimal weights in province i. The weights are derived from province-level agreement with NFI plots, and constrained by $w_{ALS,\ province\ i} + w_{GEDI,\ province\ i} = 1$. This fusion strategy leverages the strengths of both models while compensating for their individual limitations, producing a more reliable and consistent canopy height dataset across Italy. By dynamically combining the two models in a location-specific manner, the BMA fusion approach improves the robustness of the final canopy height estimates.

3.2.2 Canopy height map fusion with BMA

Once the optimal weights for each province were computed using 2015 NFI data, they were used to fuse annual predictions from both UNET models over the 2004–2024 period (**Figure 1b**). Specifically, first, canopy height maps for each year were produced independently using both the ALS-Landsat based and GEDI-Landsat based models. These were then fused using the BMA weights at the provincial level to create a harmonized annual time series.

3.3 Disturbance detection

Following the generation of the BMA-fused annual canopy height maps, we derived a canopy height reduction-based disturbance product by identifying substantial interannual reductions in canopy height of at least 5 meters, signaling potential forest disturbances. This threshold was chosen based on the model's RMSE (**Figure 2**) to balance detection sensitivity and reliability. While applying a larger threshold enhances the confidence in detected disturbances, it may also result in fewer events being identified.

A disturbance was defined as a 30 × 30 m pixel—or cluster of adjacent pixels—exhibiting a canopy height loss greater than 5 meters between a reference year (t) and the following year (t+1). To reduce false detections caused by Landsat image artifacts such as cloud cover, seasonal snow, or shadow effects, the height reduction was required to persist into the second subsequent year (t+2). This persistence criterion assumes that a true maximum canopy height reduction of more than 5 meters is unlikely to regenerate within one year, thereby enhancing the robustness of disturbance detection.

https://doi.org/10.5194/essd-2025-378
Preprint. Discussion started: 8 September 2025

It is important to note that disturbances smaller than a Landsat pixel (30 m) or partial canopy removals that do not reduce the maximum canopy height by more than 5 m cannot be consistently detected by our approach. As a result, selective logging, thinning, or low-intensity disturbances may be underrepresented in our disturbance product. This limitation is inherent to the spatial resolution of Landsat imagery and our maximum-height-based detection strategy. Nevertheless, the method captures stand-replacing disturbances and large-scale partial events that are most relevant for national forest monitoring and carbon accounting. For finer-scale management applications, integration with higher-resolution data (e.g., Sentinel-2) would be required.

3.4 External validation

3.4.1 External Validation of canopy height product

To assess the generalizability of the ALS-Landsat based and GEDI-Landsat based UNET models and the BMA fusion model, we conducted external validation using canopy height observations from the last available NFI data of Italy (Gasparini and Di Cosmo, 2015; Gasparini and Floris, 2022; National Inventory of Forests and forest Carbon pools - INFC, 2025). Each model was used to generate a canopy height map of Italy for the year 2015 (**Figure S6**). Model predictions were extracted at the geographic coordinates of NFI plots and compared to the corresponding maximum canopy height values reported in the NFI dataset (**Figure 2**). This independent assessment enabled us to evaluate how well the models generalize to field-based measurements, thereby supporting their applicability for operational forest monitoring and ecosystem modeling.

To evaluate the accuracy of BMA fusion model across other years, we randomly sampled maximum 10,000 non-zero pixels from the ALS and GEDI testing datasets for each year. The corresponding BMA predictions were extracted and compared with sampled ALS or GEDI values.

We further evaluated the BMA canopy height product by comparing the BMA estimates against the global canopy height map for 2020 by Lang et al. (Lang et al., 2023), and the European-scale products for 2019 by Turubanova et al. (Turubanova et al., 2023) and by Liu et al. (Liu et al., 2023). To evaluate agreement and consistency, we randomly sampled 50,000 non-zero pixels across Italy and compared canopy height values across corresponding locations in each product.

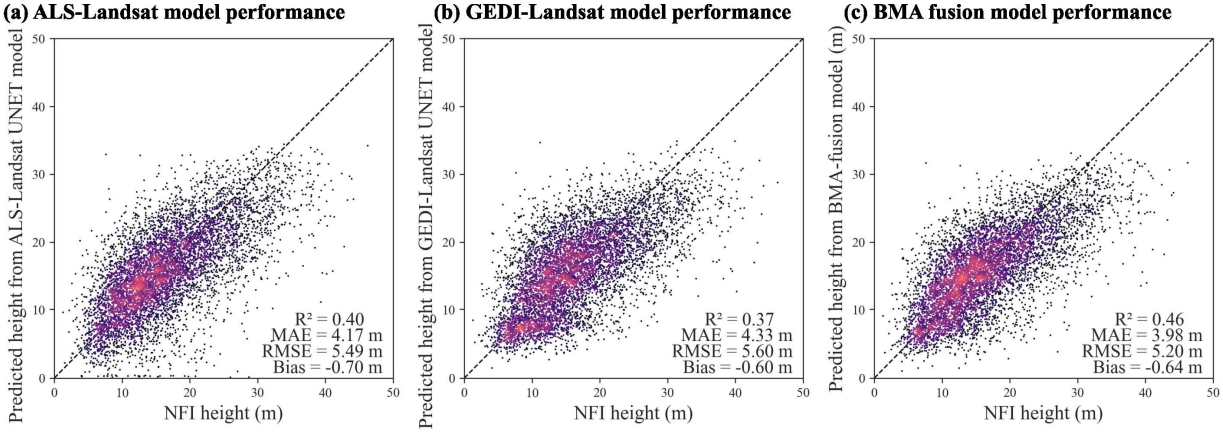

Figure 2 | External validation of ALS-Landsat, GEDI-Landsat based UNET model, and BMA fusion model using NFI data in 2015*. Plot a is scatterplot of predicted canopy heights of our ALS-Landsat based UNET canopy height model versus the canopy height of NFI observations in 2015. Plot b is scatterplot of predicted canopy heights of our GEDI-Landsat based UNET canopy height model versus the canopy height of NFI observations in 2015. Plot c is scatterplot of predicted canopy heights of our BMA fusion canopy height model versus the canopy height of NFI observations in 2015.*

https://doi.org/10.5194/essd-2025-378
Preprint. Discussion started: 8 September 2025

3.4.2 External Validation of height derived disturbance product

To evaluate the accuracy of the canopy height change-based disturbance detection, we compared our disturbance product against reference disturbance datasets (Monitoring clearcutting and subsequent rapid recovery in Mediterranean coppice forests with Landsat time series. Zenodo repository. [dataset]., 2025; Chirici et al., 2020; Francini et al., 2021, 2022) within the survey area. We assessed performance using precision, defined as the proportion of detected disturbances that were confirmed by the reference data. A disturbance identified by our product was considered a true positive (TP) if it also appeared in the reference dataset; otherwise, it was classified as a false positive (FP). Precision was then calculated as: Precision = TP / (TP + FP).

We also compared our disturbance product with those developed by Saverio et al. (Francini and Chirici, 2022), as well as the product presented in the studies by Viana-Soto et al. (Viana-Soto and Senf, 2024). To assess the precision, a random sample of 1,000 discrete disturbance patches (each >0.5 ha) from our map was compared with those identified by reference products (Francini and Chirici, 2022; Viana-Soto and Senf, 2024) over a comparable time window. Similarly, we performed a reciprocal comparison by random sampling 1,000 disturbances from reference products and evaluating their presence in our results. We calculated the proportion of events jointly detected, uniquely detected by our product, and uniquely detected by the reference datasets. This multi-source validation helps demonstrate the reliability of our disturbance mapping approach, while avoiding dependence on a single reference dataset.

4 Results

4.1 Italy canopy height map at 30m resolution covering the last two decades

We produced 30 m resolution canopy height maps of Italy over 2004-2024 using BMA to fuse predictions from two UNET models trained on ALS-Landsat and GEDI-Landsat data. The resulting national-scale map of 2024 is shown in **Figure 3a**, while plots b-g illustrate the map's ability to capture detailed forest landscape features across diverse land use types, as verified against Landsat imagery. These examples highlight the model's capacity to detect canopy height variation in a range of environments.

Using this canopy height map, we also derived a tree line map (**Figure S7**), defined as the highest elevation at which trees are present. Our results indicate that tree lines in Italy typically range between 1800 m and 2500 m above sea level, with higher elevations observed in the northern Alps compared to the southern Apennines and volcanic slopes of southern Italy, such as Mount Etna in Sicily. These spatial variations likely reflect a combination of climatic gradients, species composition, and local environmental conditions, consistent with established knowledge on tree line ecology (Körner, 2012).

https://doi.org/10.5194/essd-2025-378
Preprint. Discussion started: 8 September 2025

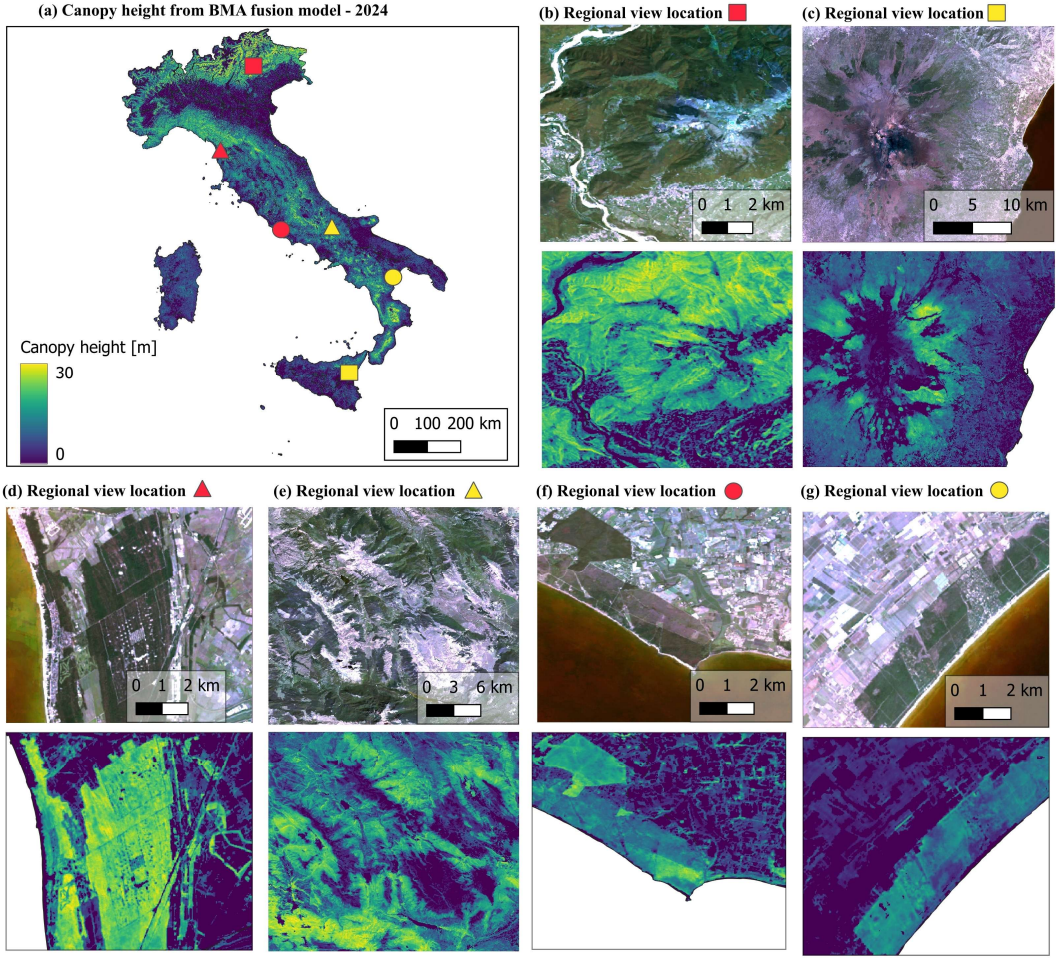

Figure 3 | Canopy height map of Italy at 30m resolution for the year 2024*. Plot a is the nationwide spatial distribution of canopy height. Plots b-g provide detailed comparisons between Landsat satellite imagery and predicted canopy height across different environments.*

To evaluate the performance of the canopy height estimation, we performed external validation using independent canopy height measurements from NFI. Predictions in 2015 from the ALS-Landsat based, GEDI-Landsat based, and BMA-fused models (**Figure S6**) were compared against maximum tree height recorded at NFI plots. The ALS-Landsat model achieved an MAE of 4.17m and R^2 of 0.4 (**Figure 2a**). The GEDI-Landsat model showed slightly lower performance, with an MAE of 4.33m and a R^2 of 0.37 (**Figure 2b**). The BMA-fused model outperformed both individual models, with an MAE of 3.98 m and R^2 of 0.46 (**Figure 2c**). We further assessed the performance of the BMA product by comparing it directly against the random sampled non-zero observations in the ALS and GEDI testing datasets. For each year, up to 10,000 observations were sampled, depending on data availability. Against ALS data in 2004-2017, the BMA model achieved an MAE of 4.09m and R^2 of 0.55 (**Figure S8a**). When compared to GEDI data in 2019-2023, the model produced a MAE of 5.11m and R^2 of 0.40 (**Figure S8b**). These evaluations confirm that the BMA fusion strategy provides balanced accuracy across multiple lidar sources.

https://doi.org/10.5194/essd-2025-378
Preprint. Discussion started: 8 September 2025

To investigate how terrain complexity influences prediction performance, we analyzed the BMA model's errors relative to slope and elevation classes, using the random sampled ALS samples (**Figure S9**). Prediction errors were generally low on gentle slopes, but increased progressively in steeper terrain, e.g., slope beyond 35°, reflecting reduced model accuracy in rugged mountainous areas (**Figure S9a**). A similar pattern was observed for elevation: errors remained low and stable up to 2000 m, but increased at higher altitudes (**Figure S9b**). These findings underscore the difficulty of accurately estimating canopy height in complex high-mountain environments, especially above 2000 m or on slopes exceeding 35°.

We further assessed our BMA canopy height estimates by comparing them with three independently developed large-scale datasets: the European-scale products from Turubanova et al. (Turubanova et al., 2023) and Liu et al. (Liu et al., 2023) in 2019, and the global canopy height map from Lang et al. (Lang et al., 2023) in 2020. Our BMA map in 2019 showed an overall good alignment with Liu's dataset (**Figure 4a, b, e, h**), with a small negative bias of −0.92 m. In contrast, when compared to Turubanova's product (**Figure 4a, b, d, g**), our BMA estimates were consistently higher, with an average positive bias of 5.16 m—indicating that Turubanova's model tends to underestimate canopy height relative to ours. Similarly, comparison with the 2020 Lang's product revealed that their model generally overestimates canopy height for trees taller than 10 m, resulting in an average negative bias of 4.19 m relative to our BMA estimates (**Figure 4h**).

To further examine these discrepancies, we compared each external product against independent GEDI canopy height observations (**Figure S10**). We randomly sampled 10,000 non-zero GEDI footprints from 2019 and 2020 and extracted corresponding canopy height estimates from Liu and Turubanova (2019) and Lang (2020). Liu's product showed a good agreement with GEDI, with a minor bias of 0.67 m. In contrast, Turubanova's estimates exhibited a substantial negative bias of −5.37 m, indicating consistent underestimation, while Lang's product showed a positive bias of +4.50 m, suggesting overestimation. Additionally, since Turubanova's dataset also includes 2015 canopy height estimates, we compared them with field measurements from the Italian National Forest Inventory (NFI). The results mirrored those from the GEDI comparison, showing an overall bias of −5.75 m (**Figure S11**), further indicating underestimation. Together, these results indicate that Liu's regional dataset aligns with GEDI and our BMA product, whereas Turubanova and Lang's models appear less accurate in capturing forest structure in Italy. Overall, the comparison supports the robustness of our BMA canopy height estimates at the national scale.

https://doi.org/10.5194/essd-2025-378
Preprint. Discussion started: 8 September 2025

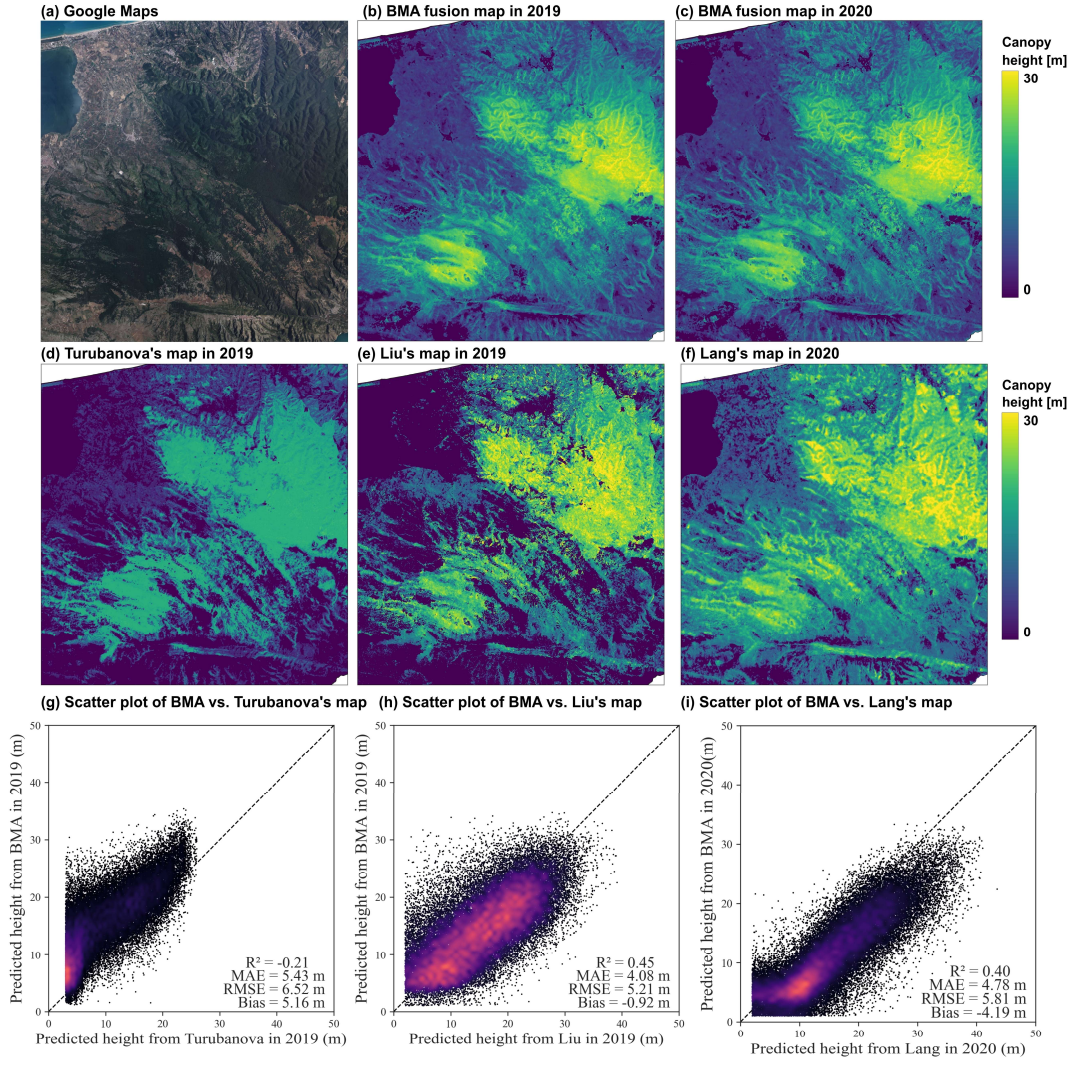

Figure 4 | Comparison between BMA products with external products from Turubanova et al. *(Turubanova et al., 2023)**, Liu et al.** (Liu et al., 2023)**and Lang et al**. (Lang et al., 2023). Plot a is the Google Maps (© Google Maps 2025) reference image in forested region in southern Italy; Plots b and c are the predicted canopy height from our BMA at this area in 2019 and 2020, respectively. Plot d is the predicted canopy height of Turubanova et al. at this area. Plot e is the predicted canopy height of Liu et al. at this area. Plot f is the predicted canopy height of Lang et al. at this area. Plot g is the scatter plot of BMA predicted canopy heights versus the canopy height from Turubanova in 2019. Plot h is the scatter plot of BMA predicted canopy heights versus the canopy height from Liu in 2019. Plot i is the scatter plot of BMA predicted canopy heights versus the canopy height from Lang in 2019.*

4.2 Disturbance map

To further validate our canopy height maps and demonstrate their practical application, we generated a disturbance map based on interannual canopy height changes. The accuracy of this product was assessed

https://doi.org/10.5194/essd-2025-378
Preprint. Discussion started: 8 September 2025

by comparing it with observed reference dataset (Monitoring clearcutting and subsequent rapid recovery in Mediterranean coppice forests with Landsat time series. Zenodo repository. [dataset]., 2025; Chirici et al., 2020; Francini et al., 2021, 2022), as shown in **Figure 5**. We showed that the range of precision is from 0.33 to 0.87 from 2005 to 2016, with an average precision of 0.64. The precision of disturbance detection ranged from 0.33 to 0.87 between 2005 and 2016, with an average precision of 0.64. Variability in precision is likely influenced by fluctuations in Landsat image quality, particularly due to the presence of clouds, shadows, and snow (Zhu and Woodcock, 2014).

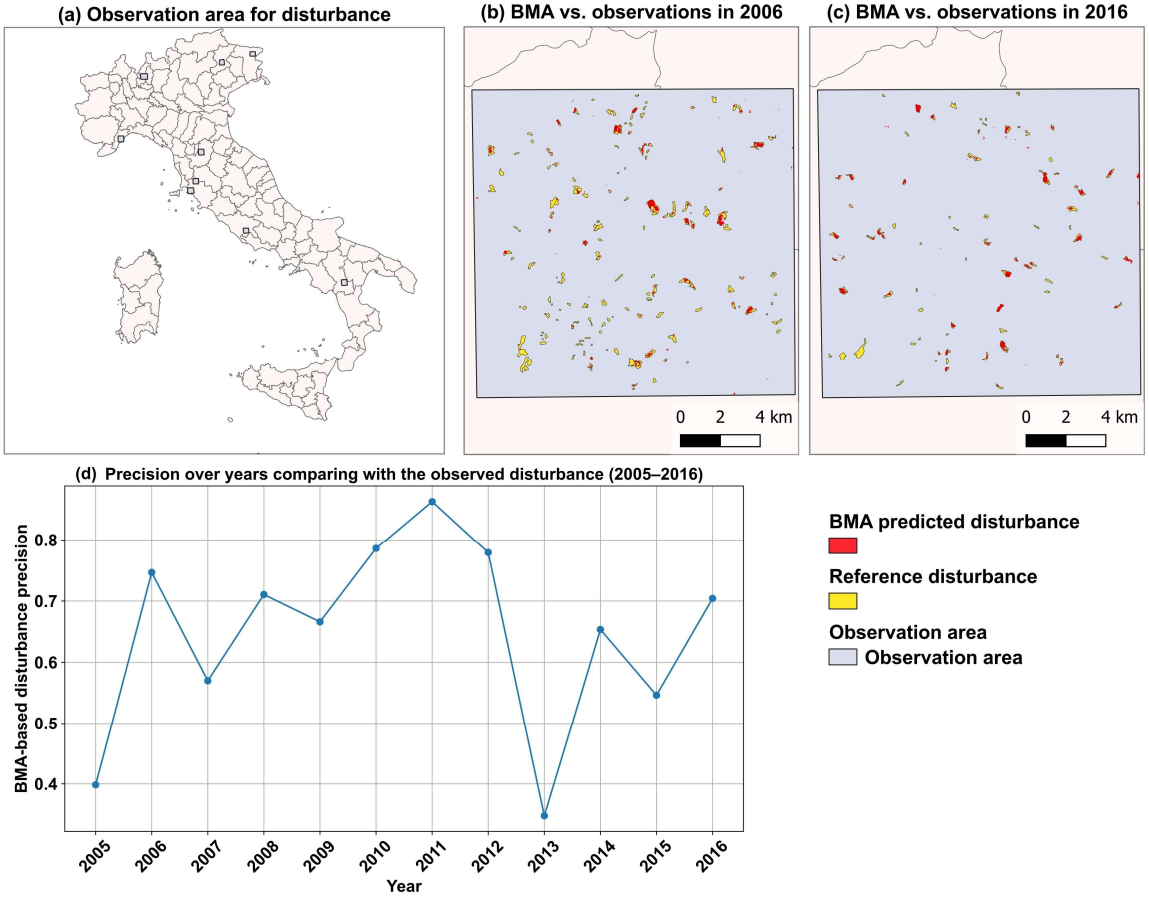

***Figure 5 | Validation of canopy height change derived forest disturbance detection using independent observations (2005–2016)**. Plot a is spatial distribution of the reference observation areas across Italy used for evaluating canopy disturbance detection. Plot b and c are the comparison of BMA-predicted disturbances (in red) with reference disturbances (in yellow) for the years 2006 and 2016 within selected observation regions. Plot d is the annual precision of BMA-based disturbance detection from 2005 to 2016, calculated as the proportion of correctly identified disturbances relative to the reference data.*

We further compared our canopy height change-based disturbance product with two independently developed datasets (Francini and Chirici, 2022; Viana-Soto and Senf, 2024). **Figure S12** shows our disturbance map in 2022-2023 alongside the Landsat-based product from Viana-Soto (Viana-Soto and Senf, 2024), while **Figure S13** presents a comparison for 2018–2019 with a Sentinel-2-based map from Saverio (Francini and Chirici, 2022). Although all three maps rely on satellite imagery, they differ in methodology:

https://doi.org/10.5194/essd-2025-378
Preprint. Discussion started: 8 September 2025

Open Access Earth System Science Data Discussions

our approach detects structural changes via canopy height reduction (>5 m), whereas the methods used by Viana-Soto and Saverio rely on spectral–temporal segmentation to classify areas as disturbed or undisturbed, with Viana-Soto further attributing disturbances to specific events such as fire, windthrow, insect outbreaks, or harvesting. Visual assessments across multiple sites (**Figure Ss 12c–i, 13c–i)** show broad agreement.

In quantitative evaluations, our disturbance map showed 59.9% overlap with Viana-Soto's product across 2,000 randomly sampled disturbance patches (≥0.5 ha), while 14.0% were uniquely detected by us and 26.1% only by Viana-Soto (**Figure S14b**). Similarly, comparison with Saverio's Sentinel-2-based product showed 54.0% agreement, with 24.4% detected only by us and 21.6% only by Saverio (**Figure S14a**). These discrepancies are probably linked to a combination of commission (false positives) and omission (false negatives) errors in all datasets. Additionally, it is important to note that not all disturbance types—such as low-intensity fires, selective logging, insect outbreaks, or windthrow—necessarily result in detectable canopy height reductions exceeding 5 m. As a result, some disturbances captured by spectral changes may not produce sufficient structural changes to be identified by our height-based approach. Conversely, our method may capture height changes from subtle or mixed disturbances that lack strong spectral signals. Integrating both structural (e.g., canopy height variation) and spectral information could enable the development of an ensemble or multi-sensor disturbance detection framework, potentially improving detection accuracy and robustness across diverse disturbance types.

Across each forest biome in Italy (**Figure S1**), we tracked post-disturbance recovery in 100 random disturbance patches from 2004–2005. Results show that canopy height recovery is most rapid in the initial years following disturbance, with the rate of regrowth gradually slowing over time. Among the biomes, Mediterranean forests exhibited the fastest recovery, followed by temperate broadleaf and mixed forests, while temperate conifer forests showed the slowest regrowth (**Figure 6**). The ability to detect disturbance and quantify subsequent regrowth underscores the value of our annual canopy-height series for assessing forest resilience and informing long-term monitoring and management.

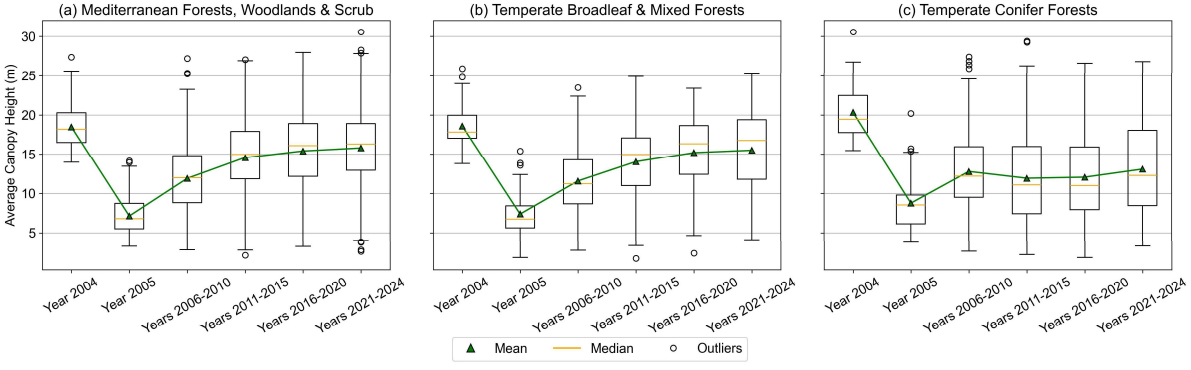

Figure 6 | Post-disturbance canopy height recovery trajectories (2004–2024) in different forest biomes in Italy*. The figure illustrates the recovery of canopy height over time in three forest biomes following disturbance events that occurred between 2004 and 2005. For each biome—(plot a) Mediterranean Forests, Woodlands & Scrub, (plot b) Temperate Broadleaf & Mixed Forests, and (plot c) Temperate Conifer Forests—100 disturbance patches were randomly sampled, and their 5-year average canopy height was tracked through 2024.*

5 Limitations and further improvements

While this study presents a novel, long-term, high-resolution canopy height and disturbance dataset for Italy, several limitations should be acknowledged:

https://doi.org/10.5194/essd-2025-378
Preprint. Discussion started: 8 September 2025

5.1 Uncertainty in extreme terrain conditions:

Despite incorporating elevation and slope data into the model, prediction errors increased in high-slope and high-altitude regions. This reflects persistent challenges in accurately modeling canopy height in rugged terrain, where terrain-induced distortions and LiDAR signal occlusions affect both training and validation.

5.2 Dependence on Landsat image quality:

Although cloud and artifact filtering were applied using QA bands and additional masking techniques, residual cloud contamination and seasonal snow may still influence Landsat reflectance values. These factors can lead to erroneous canopy height predictions or false disturbance detections in isolated cases.

5.3 BMA fusion relies on 2015 NFI reference only:

The BMA fusion weights were calibrated using NFI plot data from 2015. While this provides a reliable spatial benchmark, the assumption that relative model performance is stable across all years may introduce bias in time periods far from the reference year.

5.4 Data limitations

Post-disturbance canopy height recovery trajectories (e.g., Figure 6) could not be validated against remeasured NFI plots, as repeated inventory measurements capturing regrowth over time were unavailable. Consequently, the recovery curves in this study should be regarded as model-based trajectories rather than empirically validated growth signals. This is an important limitation that future work could address by incorporating multi-temporal ground inventory data or harmonized European networks to provide direct benchmarks for post-disturbance recovery.

5.5 Resolution limitations

The disturbance detection framework is constrained by the 30 m spatial resolution of Landsat imagery and the requirement of a $\geqslant$5 m canopy height reduction. As a result, sub-pixel or low-intensity disturbances—such as selective logging or thinning—cannot be reliably detected (see Section 3.3).

6 Data availability

The maps from 2004 to 2024 (https://doi.org/10.5281/zenodo.15627897), along with the covering 2005 to 2023 (https://doi.org/10.5281/zenodo.15627927), are publicly available on Zenodo (Canopy height map in Italy - 2004-2024 [Dataset]. Zenodo., 2025; Canopy height change derived disturbance map in Italy - 2005-2023 [Dataset]. Zenodo., 2025).

7 Conclusions

We present a long-term (2004–2024), 30 m resolution canopy height dataset for Italy, developed by fusing ALS-Landsat and GEDI-Landsat based UNET models through a Bayesian model averaging framework. The fusion approach balances the strengths of each data source, producing spatially continuous and temporally consistent canopy height estimates. Using interannual canopy height change, we also generated annual disturbance maps from 2005 to 2023. Validation against NFI data shows robust accuracy (R^2 = 0.46, MAE = 3.98 m in 2015), while comparison with observed events indicates reliable detection of stand-replacing disturbances (≥5 m canopy height loss, average precision = 0.64). The dataset also reveals biome-specific recovery trajectories, with faster regrowth in Mediterranean than in temperate coniferous forests.

This dataset provides the first spatially consistent, two-decade record of canopy height dynamics in Italy, supporting national forest monitoring, carbon accounting, climate reporting, and ecological studies on disturbance and resilience. Two main limitations remain: (i) sub-pixel or low-intensity disturbances (e.g., selective logging, thinning) are not detectable at 30 m resolution, and (ii) post-disturbance recovery

https://doi.org/10.5194/essd-2025-378
Preprint. Discussion started: 8 September 2025

trajectories are model-based and lack validation with repeated NFI plots. Addressing these gaps will require higher-resolution remote sensing (e.g., Sentinel-2, UAV lidar) and multi-temporal ground inventories.

The framework is scalable to continental or global domains by leveraging upcoming lidar missions (e.g., GEDI follow-on, ICESat-2 synergy) and dense optical archives. All datasets are openly available on Zenodo, offering a valuable resource for forest monitoring, carbon accounting, and land-use change studies.

Code Availability

The code that used in this study can be found in Figshare (https://doi.org/10.6084/m9.figshare.29416658) (Code used in the study - "A fused canopy height map of Italy (2004–2024) from spaceborne and airborne LiDAR, and Landsat via deep learning and Bayesian averaging ", 2025).

Disclaimer

Publisher's note: Copernicus Publications remains neutral with regard to jurisdictional claims made in the text, published maps, institutional affiliations, or any other geographical representation in this paper. While Copernicus Publications makes every effort to include appropriate place names, the final responsibility lies with the authors.

Acknowledgement

This work was supported by the ANR under the AI4Forests program with the reference ANR-22-FAI1-0002. YS, PC, MS, IF and AD are supported by the French German project AI4FOREST (ANR-22-FAI1-0002-01) funded by ANR and DLR. This research includes data from the Global Ecosystem Dynamics Investigation (GEDI), distributed by NASA's Land Processes Distributed Active Archive Center (LP DAAC).

This study was also partially supported via the following projects: 1. MULTIFOR "Multi-scale observations to predict Forest response to pollution and climate change" PRIN 2020 Research Project of National Relevance funded by the Italian Ministry of University and Research (prot. 2020E52THS). 2. SUPERB "Systemic solutions for upscaling of urgent ecosystem restoration for forest related biodiversity and ecosystem services" H2020 project funded by the European Commission, number 101036849 call LC-GD-7-1-2020. 3. FORWARDS "The ForestWard Observatory to Secure Resilience of European Forests", HORIZON project funded by the European Commission, number 101084481 call HORIZON-CL6-2022-CLIMATE-01. 4. MONIFUN. H2020 project funded by the European Commission, number 101134991 call HORIZON-CL6-2023-CircBio-01-14. 5. NextGenCarbon. H2020 project funded by the European Commission, number 101184989 call HORIZON-CL5-2024-D1-01-07. NBFC "National Biodiversity Future Center" project funded under the National Recovery and Resilience Plan (NRRP), NextGenerationEU; Project code CN_00000033, adopted by the Italian Ministry of University and Research, CUP B83C22002930006. 6. Space It Up. Project funded by the Italian Space Agency and the Ministry of University and Research - Contract No. 2024-5-E.0 - CUP No. I53D24000060005. 7. Interdisciplinary program ARTEMIS of Lorraine Université d'Excellence (ANR-15-IDEX-04-LUE).

This research uses Landsat 5 Thematic Mapper, Landsat 7 Enhanced Thematic Mapper Plus, and Landsat 8 Operational Land Imager data distributed by the U.S. Geological Survey (USGS), and Global Ecosystem Dynamics Investigation (GEDI) data distributed by NASA's Land Processes Distributed Active Archive Center (LP DAAC). All datasets were accessed and processed via Google Earth Engine. The ALS and NFI data were acquired under the help of Dr. Saverio Francini and Dr. Giovanni Forzieri. Other datasets used in this study are open-access and freely available, including those from GEDI, Landsat, Liu, Lang, Turubanova, Saverio, and Viana-Soto.

https://doi.org/10.5194/essd-2025-378
Preprint. Discussion started: 8 September 2025

We acknowledge the use of Google Maps satellite imagery (© Google Maps 2025), accessed via QGIS, which was used solely for academic, non-commercial purposes to support geographic visualization and spatial referencing in this study.

Author Contributions

Conceptualization: YS, MS, IF, PC

Methodology: YS, MS, IF, PC, NB

Investigation: YS, AP, SB

Visualization: YS, XZ, YX, KY, HC, SC

Data acquisition: YS, SF, GF

Funding acquisition: PC, AA

Supervision: YS, PC, AA

Writing—original draft: YS, PC

Writing—review & editing: YS, MS, IF, PC, NB, XZ, SC, HC, AA, SB, AP, KY, SF, GF

Competing Interests.

None declared.

https://doi.org/10.5194/essd-2025-378
Preprint. Discussion started: 8 September 2025

Reference

Besic, N., Picard, N., Vega, C., Bontemps, J.-D., Hertzog, L., Renaud, J.-P., Fogel, F., Schwartz, M., Pellissier-Tanon, A., Destouet, G., Mortier, F., Planells-Rodriguez, M., and Ciais, P.: Remote-sensing-based forest canopy height mapping: some models are useful, but might they provide us with even more insights when combined?, Geosci Model Dev, 18, 337–359, https://doi.org/10.5194/gmd-18-337-2025, 2025.

Budei, B. C., St-Onge, B., Hopkinson, C., and Audet, F.-A.: Identifying the genus or species of individual trees using a three-wavelength airborne lidar system, Remote Sens Environ, 204, 632–647, https://doi.org/10.1016/j.rse.2017.09.037, 2018.

Canopy height change derived disturbance map in Italy - 2005-2023 [Dataset]. Zenodo.: https://doi.org/10.5281/zenodo.15627927, last access: 30 June 2025.

Canopy height map in Italy - 2004-2024 [Dataset]. Zenodo.: https://doi.org/10.5281/zenodo.15627897, last access: 30 June 2025.

Chave, J., Réjou-Méchain, M., Búrquez, A., Chidumayo, E., Colgan, M. S., Delitti, W. B. C., Duque, A., Eid, T., Fearnside, P. M., Goodman, R. C., Henry, M., Martínez-Yrízar, A., Mugasha, W. A., Muller-Landau, H. C., Mencuccini, M., Nelson, B. W., Ngomanda, A., Nogueira, E. M., Ortiz-Malavassi, E., Pélissier, R., Ploton, P., Ryan, C. M., Saldarriaga, J. G., and Vieilledent, G.: Improved allometric models to estimate the aboveground biomass of tropical trees, Glob Chang Biol, 20, 3177–3190, https://doi.org/10.1111/gcb.12629, 2014.

Chen, S., Mulder, V. L., Heuvelink, G. B. M., Poggio, L., Caubet, M., Román Dobarco, M., Walter, C., and Arrouays, D.: Model averaging for mapping topsoil organic carbon in France, Geoderma, 366, 114237, https://doi.org/10.1016/j.geoderma.2020.114237, 2020.

Chirici, G., Giannetti, F., Mazza, E., Francini, S., Travaglini, D., Pegna, R., and White, J. C.: Monitoring clearcutting and subsequent rapid recovery in Mediterranean coppice forests with Landsat time series, Ann For Sci, 77, 40, https://doi.org/10.1007/s13595-020-00936-2, 2020.

Code used in the study - "A fused canopy height map of Italy (2004–2024) from spaceborne and airborne LiDAR, and Landsat via deep learning and Bayesian averaging ": https://doi.org/10.6084/m9.figshare.29416658, last access: 3 July 2025.

Cohen, W. B., Yang, Z., and Kennedy, R.: Detecting trends in forest disturbance and recovery using yearly Landsat time series: 2. TimeSync — Tools for calibration and validation, Remote Sens Environ, 114, 2911–2924, https://doi.org/10.1016/j.rse.2010.07.010, 2010.

Coops, N. C., Tompalski, P., Goodbody, T. R. H., Queinnec, M., Luther, J. E., Bolton, D. K., White, J. C., Wulder, M. A., van Lier, O. R., and Hermosilla, T.: Modelling lidar-derived estimates of forest attributes over space and time: A review of approaches and future trends, Remote Sens Environ, 260, 112477, https://doi.org/10.1016/j.rse.2021.112477, 2021.

Crawford, C. J., Roy, D. P., Arab, S., Barnes, C., Vermote, E., Hulley, G., Gerace, A., Choate, M., Engebretson, C., Micijevic, E., Schmidt, G., Anderson, C., Anderson, M., Bouchard, M., Cook, B., Dittmeier, R., Howard, D., Jenkerson, C., Kim, M., Kleyians, T., Maiersperger, T., Mueller, C., Neigh, C., Owen, L., Page, B., Pahlevan, N., Rengarajan, R., Roger, J.-C., Sayler, K., Scaramuzza, P., Skakun, S., Yan, L., Zhang, H. K., Zhu, Z., and Zahn, S.: The 50-year Landsat collection 2 archive, Science of Remote Sensing, 8, 100103, https://doi.org/10.1016/j.srs.2023.100103, 2023.

D'Amico, G., Vangi, E., Francini, S., Giannetti, F., Nicolaci, A., Travaglini, D., Massai, L., Giambastiani, Y., Terranova, C., and Chirici, G.: Are we ready for a National Forest Information System? State of the art of forest maps and airborne laser scanning data availability in Italy, IForest, 14, 144–154, https://doi.org/10.3832/ifor3648-014, 2021.

https://doi.org/10.5194/essd-2025-378
Preprint. Discussion started: 8 September 2025

Duan, Q., Ajami, N. K., Gao, X., and Sorooshian, S.: Multi-model ensemble hydrologic prediction using Bayesian model averaging, Adv Water Resour, 30, 1371–1386, https://doi.org/10.1016/j.advwatres.2006.11.014, 2007.

Dubayah, R., Blair, J. B., Goetz, S., Fatoyinbo, L., Hansen, M., Healey, S., Hofton, M., Hurtt, G., Kellner, J., Luthcke, S., Armston, J., Tang, H., Duncanson, L., Hancock, S., Jantz, P., Marselis, S., Patterson, P. L., Qi, W., and Silva, C.: The Global Ecosystem Dynamics Investigation: High-resolution laser ranging of the Earth's forests and topography, Science of Remote Sensing, 1, 100002, https://doi.org/10.1016/j.srs.2020.100002, 2020.

Dubayah, R., Hofton, M., Blair, J., Armston, J., Tang, H., and Luthcke, S.: GEDI L2A Elevation and Height Metrics Data Global Footprint Level V002 [Data set], NASA Land Processes Distributed Active Archive Center, 2021.

Fayad, I., Ciais, P., Schwartz, M., Wigneron, J.-P., Baghdadi, N., de Truchis, A., d'Aspremont, A., Frappart, F., Saatchi, S., Sean, E., Pellissier-Tanon, A., and Bazzi, H.: Hy-TeC: a hybrid vision transformer model for high-resolution and large-scale mapping of canopy height, Remote Sens Environ, 302, 113945, https://doi.org/10.1016/j.rse.2023.113945, 2024.

Francini, S. and Chirici, G.: A Sentinel-2 derived dataset of forest disturbances occurred in Italy between 2017 and 2020, Data Brief, 42, 108297, https://doi.org/10.1016/j.dib.2022.108297, 2022.

Francini, S., McRoberts, R. E., Giannetti, F., Mencucci, M., Marchetti, M., Scarascia Mugnozza, G., and Chirici, G.: Near-real time forest change detection using PlanetScope imagery, Eur J Remote Sens, 53, 233–244, https://doi.org/10.1080/22797254.2020.1806734, 2020.

Francini, S., McRoberts, R. E., Giannetti, F., Marchetti, M., Scarascia Mugnozza, G., and Chirici, G.: The Three Indices Three Dimensions (3I3D) algorithm: a new method for forest disturbance mapping and area estimation based on optical remotely sensed imagery, Int J Remote Sens, 42, 4693–4711, https://doi.org/10.1080/01431161.2021.1899334, 2021.

Francini, S., D'Amico, G., Vangi, E., Borghi, C., and Chirici, G.: Integrating GEDI and Landsat: Spaceborne Lidar and Four Decades of Optical Imagery for the Analysis of Forest Disturbances and Biomass Changes in Italy, Sensors, 22, 2015, https://doi.org/10.3390/s22052015, 2022.

Francini, S., Hermosilla, T., Coops, N. C., Wulder, M. A., White, J. C., and Chirici, G.: An assessment approach for pixel-based image composites, ISPRS Journal of Photogrammetry and Remote Sensing, 202, 1–12, https://doi.org/10.1016/j.isprsjprs.2023.06.002, 2023.

Gasparini, P. and Di Cosmo, L.: Forest carbon in Italian forests: Stocks, inherent variability and predictability using NFI data, For Ecol Manage, 337, 186–195, https://doi.org/10.1016/j.foreco.2014.11.012, 2015.

Gasparini, P. and Floris, A.: Definitions and Sampling Design, 17–48, https://doi.org/10.1007/978-3-030-98678-0_2, 2022.

ee.Terrain.slope: https://developers.google.com/earth-engine/apidocs/ee-terrain-slope, last access: 8 June 2025.

Landsat Algorithms: https://developers.google.com/earth-engine/guides/landsat#landsat-processing-methods, last access: 8 June 2025.

Landsat ETM+ to OLI Harmonization: https://developers.google.com/earth-engine/tutorials/community/landsat-etm-to-oli-harmonization, last access: 8 June 2025.

Hansen, M. C., Potapov, P. V., Moore, R., Hancher, M., Turubanova, S. A., Tyukavina, A., Thau, D., Stehman, S. V., Goetz, S. J., Loveland, T. R., Kommareddy, A., Egorov, A., Chini, L., Justice, C. O., and

https://doi.org/10.5194/essd-2025-378
Preprint. Discussion started: 8 September 2025

Townshend, J. R. G.: High-Resolution Global Maps of 21st-Century Forest Cover Change, Science (1979), 342, 850–853, https://doi.org/10.1126/science.1244693, 2013a.

Hansen, M. C., Potapov, P. V., Moore, R., Hancher, M., Turubanova, S. A., Tyukavina, A., Thau, D., Stehman, S. V., Goetz, S. J., Loveland, T. R., Kommareddy, A., Egorov, A., Chini, L., Justice, C. O., and Townshend, J. R. G.: High-Resolution Global Maps of 21st-Century Forest Cover Change, Science (1979), 342, 850–853, https://doi.org/10.1126/science.1244693, 2013b.

Hermosilla, T., Wulder, M. A., White, J. C., Coops, N. C., and Hobart, G. W.: An integrated Landsat time series protocol for change detection and generation of annual gap-free surface reflectance composites, Remote Sens Environ, 158, 220–234, https://doi.org/10.1016/j.rse.2014.11.005, 2015.

Hoeting, J. A., Madigan, D., Raftery, A. E., and Volinsky, C. T.: Bayesian Model Averaging: A Tutorial, Statistical Science, 14, 382–401, 1999.

Kaewmanee, M., Leigh, L., Shah, R., and Gross, G.: Inter-Comparison of Landsat-8 and Landsat-9 during On-Orbit Initialization and Verification (OIV) Using Extended Pseudo Invariant Calibration Sites (EPICS): Advanced Methods, Remote Sens (Basel), 15, 2330, https://doi.org/10.3390/rs15092330, 2023.

KC, K., Zhao, K., Romanko, M., and Khanal, S.: Assessment of the Spatial and Temporal Patterns of Cover Crops Using Remote Sensing, Remote Sens (Basel), 13, 2689, https://doi.org/10.3390/rs13142689, 2021.

Kennedy, R. E., Yang, Z., and Cohen, W. B.: Detecting trends in forest disturbance and recovery using yearly Landsat time series: 1. LandTrendr — Temporal segmentation algorithms, Remote Sens Environ, 114, 2897–2910, https://doi.org/10.1016/j.rse.2010.07.008, 2010.

Körner, C.: Alpine Treelines, Springer Basel, Basel, https://doi.org/10.1007/978-3-0348-0396-0, 2012.

Kovalskyy, V. and Roy, D. P.: The global availability of Landsat 5 TM and Landsat 7 ETM+ land surface observations and implications for global 30m Landsat data product generation, Remote Sens Environ, 130, 280–293, https://doi.org/10.1016/j.rse.2012.12.003, 2013.

Kutchartt, E., Pedron, M., and Pirotti, F.: ASSESSMENT OF CANOPY AND GROUND HEIGHT ACCURACY FROM GEDI LIDAR OVER STEEP MOUNTAIN AREAS, ISPRS Annals of the Photogrammetry, Remote Sensing and Spatial Information Sciences, V-3–2022, 431–438, https://doi.org/10.5194/isprs-annals-V-3-2022-431-2022, 2022.

Lang, N., Jetz, W., Schindler, K., and Wegner, J. D.: A high-resolution canopy height model of the Earth, Nat Ecol Evol, 7, 1778–1789, https://doi.org/10.1038/s41559-023-02206-6, 2023.

Liu, S., Brandt, M., Nord-Larsen, T., Chave, J., Reiner, F., Lang, N., Tong, X., Ciais, P., Igel, C., Pascual, A., Guerra-Hernandez, J., Li, S., Mugabowindekwe, M., Saatchi, S., Yue, Y., Chen, Z., and Fensholt, R.: The overlooked contribution of trees outside forests to tree cover and woody biomass across Europe, Sci Adv, 9, https://doi.org/10.1126/sciadv.adh4097, 2023.

Monitoring clearcutting and subsequent rapid recovery in Mediterranean coppice forests with Landsat time series. Zenodo repository. [dataset]. https://doi.org/10.5281/zenodo.3689194, 2020.

Montaghi, A., Corona, P., Dalponte, M., Gianelle, D., Chirici, G., and Olsson, H.: Airborne laser scanning of forest resources: An overview of research in Italy as a commentary case study, International Journal of Applied Earth Observation and Geoinformation, 23, 288–300, https://doi.org/10.1016/j.jag.2012.10.002, 2013.

National Inventory of Forests and forest Carbon pools - INFC: https://www.inventarioforestale.org/en/, last access: 8 June 2025.

Optech, Gemini Airborne Sensors, n.d. https://cp1.inkrefuge.com/admin/asset/uploads/302/portfolio/pdf/gemini-brochure.pdf.

https://doi.org/10.5194/essd-2025-378
Preprint. Discussion started: 8 September 2025

Palahí, M., Valbuena, R., Senf, C., Acil, N., Pugh, T. A. M., Sadler, J., Seidl, R., Potapov, P., Gardiner, B., Hetemäki, L., Chirici, G., Francini, S., Hlásny, T., Lerink, B. J. W., Olsson, H., González Olabarria, J. R., Ascoli, D., Asikainen, A., Bauhus, J., Berndes, G., Donis, J., Fridman, J., Hanewinkel, M., Jactel, H., Lindner, M., Marchetti, M., Marušák, R., Sheil, D., Tomé, M., Trasobares, A., Verkerk, P. J., Korhonen, M., and Nabuurs, G.-J.: Concerns about reported harvests in European forests, Nature, 592, E15–E17, https://doi.org/10.1038/s41586-021-03292-x, 2021.

Pauls, J., Zimmer, M., Kelly, U. M., Schwartz, M., Saatchi, S., Ciais, P., Pokutta, S., Brandt, M., and Gieseke, F.: Estimating Canopy Height at Scale, in: Proceedings of the 41st International Conference on Machine Learning, 39972–39988, 2024.

Pirotti, F.: Assessing a Template Matching Approach for Tree Height and Position Extraction from Lidar-Derived Canopy Height Models of Pinus Pinaster Stands, Forests, 1, 194–208, https://doi.org/10.3390/f1040194, 2010.

Potapov, P., Li, X., Hernandez-Serna, A., Tyukavina, A., Hansen, M. C., Kommareddy, A., Pickens, A., Turubanova, S., Tang, H., Silva, C. E., Armston, J., Dubayah, R., Blair, J. B., and Hofton, M.: Mapping global forest canopy height through integration of GEDI and Landsat data, Remote Sens Environ, 253, 112165, https://doi.org/10.1016/j.rse.2020.112165, 2021.

Rajab Pourrahmati, M., Baghdadi, N., Scolforo, H. F., Alvares, C. A., Stape, J. L., Fayad, I., and le Maire, G.: Integration of very high-resolution stereo satellite images and airborne or satellite Lidar for Eucalyptus canopy height estimation, Science of Remote Sensing, 10, 100170, https://doi.org/10.1016/j.srs.2024.100170, 2024.

Ronneberger, O., Fischer, P., and Brox, T.: U-Net: Convolutional Networks for Biomedical Image Segmentation, 234–241, https://doi.org/10.1007/978-3-319-24574-4_28, 2015.

Roy, D. P., Wulder, M. A., Loveland, T. R., C.E., W., Allen, R. G., Anderson, M. C., Helder, D., Irons, J. R., Johnson, D. M., Kennedy, R., Scambos, T. A., Schaaf, C. B., Schott, J. R., Sheng, Y., Vermote, E. F., Belward, A. S., Bindschadler, R., Cohen, W. B., Gao, F., Hipple, J. D., Hostert, P., Huntington, J., Justice, C. O., Kilic, A., Kovalskyy, V., Lee, Z. P., Lymburner, L., Masek, J. G., McCorkel, J., Shuai, Y., Trezza, R., Vogelmann, J., Wynne, R. H., and Zhu, Z.: Landsat-8: Science and product vision for terrestrial global change research, Remote Sens Environ, 145, 154–172, https://doi.org/10.1016/j.rse.2014.02.001, 2014.

Roy, D. P., Kovalskyy, V., Zhang, H. K., Vermote, E. F., Yan, L., Kumar, S. S., and Egorov, A.: Characterization of Landsat-7 to Landsat-8 reflective wavelength and normalized difference vegetation index continuity, Remote Sens Environ, 185, 57–70, https://doi.org/10.1016/j.rse.2015.12.024, 2016.

Savage, S., Lawrence, R., Squires, J., Holbrook, J., Olson, L., Braaten, J., and Cohen, W.: Shifts in Forest Structure in Northwest Montana from 1972 to 2015 Using the Landsat Archive from Multispectral Scanner to Operational Land Imager, Forests, 9, 157, https://doi.org/10.3390/f9040157, 2018.

Schleich, A., Durrieu, S., Soma, M., and Vega, C.: Improving GEDI Footprint Geolocation Using a High-Resolution Digital Elevation Model, IEEE J Sel Top Appl Earth Obs Remote Sens, 16, 7718–7732, https://doi.org/10.1109/JSTARS.2023.3298991, 2023.

Schwartz, M., Ciais, P., De Truchis, A., Chave, J., Ottlé, C., Vega, C., Wigneron, J.-P., Nicolas, M., Jouaber, S., Liu, S., Brandt, M., and Fayad, I.: FORMS: Forest Multiple Source height, wood volume, and biomass maps in France at 10 to 30 m resolution based on Sentinel-1, Sentinel-2, and Global Ecosystem Dynamics Investigation (GEDI) data with a deep learning approach, Earth Syst Sci Data, 15, 4927–4945, https://doi.org/10.5194/essd-15-4927-2023, 2023.

Selvi, F., Campetella, G., Canullo, R., Chelli, S., Domina, G., Farris, E., Gasperini, C., Rosati, L., Wellstein, C., and Carrari, E.: The Italian endemic forest plants: an annotated inventory and synthesis of knowledge, Plant Ecol Evol, 156, 29–45, https://doi.org/10.5091/plecevo.95929, 2023.

https://doi.org/10.5194/essd-2025-378
Preprint. Discussion started: 8 September 2025

Shukla, P. R., Skea, J., Buendia, E. C., Masson-Delmotte, V., Pörtner, H.-O., Roberts, D. C., Zhai, P., Slade, R., Connors, S., Diemen, R. van, Ferrat, M., Haughey, E., Luz, S., Neogi, S., Pathak, M., Petzold, J., Pereira, J. P., Vyas, P., Huntley, E., Kissick, K., Belkacemi, M., and Malley, J.: IPCC, 2019: Summary for Policymakers. In: Climate Change and Land: an IPCC special report on climate change, desertification, land degradation, sustainable land management, food security, and greenhouse gas fluxes in terrestrial ecosystems, n.d.

Solórzano, J. V., Mas, J. F., Gao, Y., and Gallardo-Cruz, J. A.: Land Use Land Cover Classification with U-Net: Advantages of Combining Sentinel-1 and Sentinel-2 Imagery, Remote Sens (Basel), 13, 3600, https://doi.org/10.3390/rs13183600, 2021.

Srivastava, N., Hinton, G., Krizhevsky, A., Sutskever, I., and Salakhutdinov, R.: Dropout: A Simple Way to Prevent Neural Networks from Overfitting, Journal of Machine Learning Research, 15, 1929–1958, 2014.

Su, Y., Schwartz, M., Fayad, I., García, M., Zavala, M. A., Tijerín-Triviño, J., Astigarraga, J., Cruz-Alonso, V., Liu, S., Zhang, X., Chen, S., Ritter, F., Besic, N., d'Aspremont, A., and Ciais, P.: Canopy height and biomass distribution across the forests of Iberian Peninsula, Sci Data, 12, 678, https://doi.org/10.1038/s41597-025-05021-9, 2025.

Tadono, T., Ishida, H., Oda, F., Naito, S., Minakawa, K., and Iwamoto, H.: Precise Global DEM Generation by ALOS PRISM, ISPRS Annals of the Photogrammetry, Remote Sensing and Spatial Information Sciences, II–4, 71–76, https://doi.org/10.5194/isprsannals-II-4-71-2014, 2014.

Tadono, T., Nagai, H., Ishida, H., Oda, F., Naito, S., Minakawa, K., and Iwamoto, H.: GENERATION OF THE 30 M-MESH GLOBAL DIGITAL SURFACE MODEL BY ALOS PRISM, The International Archives of the Photogrammetry, Remote Sensing and Spatial Information Sciences, XLI-B4, 157–162, https://doi.org/10.5194/isprs-archives-XLI-B4-157-2016, 2016.

Takaku, J., Tadono, T., and Tsutsui, K.: Generation of High Resolution Global DSM from ALOS PRISM, The International Archives of the Photogrammetry, Remote Sensing and Spatial Information Sciences, XL–4, 243–248, https://doi.org/10.5194/isprsarchives-XL-4-243-2014, 2014.

Takaku, J., Tadono, T., Tsutsui, K., and Ichikawa, M.: VALIDATION OF "AW3D" GLOBAL DSM GENERATED FROM ALOS PRISM, ISPRS Annals of the Photogrammetry, Remote Sensing and Spatial Information Sciences, III–4, 25–31, https://doi.org/10.5194/isprs-annals-III-4-25-2016, 2016.

Turubanova, S., Potapov, P., Hansen, M. C., Li, X., Tyukavina, A., Pickens, A. H., Hernandez-Serna, A., Arranz, A. P., Guerra-Hernandez, J., Senf, C., Häme, T., Valbuena, R., Eklundh, L., Brovkina, O., Navrátilová, B., Novotný, J., Harris, N., and Stolle, F.: Tree canopy extent and height change in Europe, 2001–2021, quantified using Landsat data archive, Remote Sens Environ, 298, 113797, https://doi.org/10.1016/j.rse.2023.113797, 2023.

USGS Landsat 5 Level 2, Collection 2, Tier 1: https://developers.google.com/earth-engine/datasets/catalog/LANDSAT_LT05_C02_T1_L2#description, last access: 8 June 2025.

USGS Landsat 7 Level 2, Collection 2, Tier 1: https://developers.google.com/earth-engine/datasets/catalog/LANDSAT_LE07_C02_T1_L2#description, last access: 8 June 2025.

USGS Landsat 8 Level 2, Collection 2, Tier 1: https://developers.google.com/earth-engine/datasets/catalog/LANDSAT_LC08_C02_T1_L2#description, last access: 8 June 2025.

Vermote, E., Justice, C., Claverie, M., and Franch, B.: Preliminary analysis of the performance of the Landsat 8/OLI land surface reflectance product, Remote Sens Environ, 185, 46–56, https://doi.org/10.1016/j.rse.2016.04.008, 2016.

Viana-Soto, A. and Senf, C.: The European Forest Disturbance Atlas: a forest disturbance monitoring system using the Landsat archive, https://doi.org/10.5194/essd-2024-361, 21 November 2024.

https://doi.org/10.5194/essd-2025-378
Preprint. Discussion started: 8 September 2025

Vogeler, J. C., Braaten, J. D., Slesak, R. A., and Falkowski, M. J.: Extracting the full value of the Landsat archive: Inter-sensor harmonization for the mapping of Minnesota forest canopy cover (1973–2015), Remote Sens Environ, 209, 363–374, https://doi.org/10.1016/j.rse.2018.02.046, 2018.

Wulder, M. A., White, J. C., Nelson, R. F., Næsset, E., Ørka, H. O., Coops, N. C., Hilker, T., Bater, C. W., and Gobakken, T.: Lidar sampling for large-area forest characterization: A review, Remote Sens Environ, 121, 196–209, https://doi.org/10.1016/j.rse.2012.02.001, 2012.

Wulder, M. A., White, J. C., Loveland, T. R., Woodcock, C. E., Belward, A. S., Cohen, W. B., Fosnight, E. A., Shaw, J., Masek, J. G., and Roy, D. P.: The global Landsat archive: Status, consolidation, and direction, Remote Sens Environ, 185, 271–283, https://doi.org/10.1016/j.rse.2015.11.032, 2016.

Xu, H., Ren, M., and Yang, L.: Evaluating the consistency of surface brightness, greenness, and wetness observations between Landsat-8 OLI and Landsat-9 OLI2 through underfly images, International Journal of Applied Earth Observation and Geoinformation, 124, 103546, https://doi.org/10.1016/j.jag.2023.103546, 2023a.

Xu, Y., Ding, S., Chen, P., Tang, H., Ren, H., and Huang, H.: Horizontal Geolocation Error Evaluation and Correction on Full-Waveform LiDAR Footprints via Waveform Matching, Remote Sens (Basel), 15, 776, https://doi.org/10.3390/rs15030776, 2023b.

ESA WorldCover 10 m 2021 v200: https://doi.org/10.5281/zenodo.7254221, last access: 11 June 2024.

Zheng, Q., Yang, M., Tian, X., Jiang, N., and Wang, D.: A Full Stage Data Augmentation Method in Deep Convolutional Neural Network for Natural Image Classification, Discrete Dyn Nat Soc, 2020, 1–11, https://doi.org/10.1155/2020/4706576, 2020.

Zhu, X. X., Tuia, D., Mou, L., Xia, G.-S., Zhang, L., Xu, F., and Fraundorfer, F.: Deep Learning in Remote Sensing: A Comprehensive Review and List of Resources, IEEE Geosci Remote Sens Mag, 5, 8–36, https://doi.org/10.1109/MGRS.2017.2762307, 2017.

Zhu, Z. and Woodcock, C. E.: Object-based cloud and cloud shadow detection in Landsat imagery, Remote Sens Environ, 118, 83–94, https://doi.org/10.1016/j.rse.2011.10.028, 2012.

Zhu, Z. and Woodcock, C. E.: Automated cloud, cloud shadow, and snow detection in multitemporal Landsat data: An algorithm designed specifically for monitoring land cover change, Remote Sens Environ, 152, 217–234, https://doi.org/10.1016/j.rse.2014.06.012, 2014.